

Small RNA driven feed-forward loop: Fine-tuning of protein synthesis through sRNA mediated cross-talk

Swathi Tej¹ and Sutapa Mukherji^{2*}

Protein Chemistry and Technology, Central Food Technological Research Institute, Mysore 570 020, Karnataka, India

(Dated: March 21, 2022)

Often in bacterial regulatory networks, small non-coding RNAs (sRNA) interact with several mRNA species. The competition among mRNAs for binding to the common pool of sRNA might lead to an effective interaction (cross-talk) between the mRNAs. This is similar to the competing endogenous RNA (ceRNA) effect wherein the competition to bind to the same pool of micro-RNA in Eukaryotes leads to micro-RNA mediated cross-talk resulting in subtle and complex gene regulation with stabilised gene expression. Here, we study an sRNA-driven feed-forward loop (sFFL) where the top-tier regulator, an sRNA, binds with two species of mRNA for their translational up-regulation. In general, in a feed-forward loop, the top-tier regulator regulates the target protein synthesis through two path ways; while one involves a direct regulation of the target protein, the other involves an indirect regulation via up- or down-regulation of an intermediate regulator of the target protein. In the present sFFL, an sRNA (RprA) translationally activates the target protein (RicI) directly and also, indirectly, via up-regulation of its transcriptional activator (σ^s). We show that the sRNA-mediated cross-talk between the two mRNA species leads to maximum target protein synthesis for low synthesis rates of σ^s -mRNA. This indicates the possibility of an optimal target protein synthesis with an efficient utilisation of σ^s -mRNA which is typically associated with various other stress response activities inside the cell. Since gene expression is inherently stochastic due to the probabilistic nature of various molecular interactions associated with it, we next quantify the fluctuations in the target protein level using generating function based approach and stochastic simulations. The coefficient of variation that provides a measure of fluctuations in the concentration shows a minimum under conditions that also correspond to optimal target protein synthesis. This prompts us to conclude that, in sFFL, the cross-talk leads to optimal target protein synthesis with minimal noise and an efficient utilisation of σ^s -mRNA.

I. INTRODUCTION

The gene expression is a complex process involving, for example, a number of genes, proteins and regulatory RNAs of different kinds. Different types of molecular mechanism at transcriptional and post-transcriptional levels regulate the gene expression process to ensure that the proteins are synthesized to the desired level with the required efficiency. Among various regulatory molecules, small noncoding RNAs (sRNAs) have drawn significant attention in the recent past for their diverse regulatory properties [1, 2]. sRNAs are approximately 50 – 300 nucleotides long and they often regulate the protein synthesis by base-pairing with the target mRNAs leading to mRNA degradation or translational inhibition [2, 3]. Although sRNA mediated interactions are found to be mostly repressing in nature, there are recent reports of activating interactions by sRNAs where sRNAs enhance the stability of mRNAs by sequestering the RNase E recognition site or facilitate translation initiation by opening the sequestered ribosome binding site of the secondary structure mRNAs [3, 4]. Since sRNAs do not code for proteins, it is generally believed that sRNAs lead to fast and energy-efficient gene regulation.

A number of interesting properties are found in the

case of sRNA mediated gene regulation. For instance, in the case of only sRNA mediated regulation, the target protein concentration shows a threshold linear response [5]. In the case of combined transcriptional and translational regulation by proteins and sRNAs, respectively, one, however, finds both monostable (with threshold linear response) and bistable regions in the target protein concentration [6]. In addition, sRNAs (or micro-RNAs (miRNA) in case of Eukaryotes) also have the ability to filter gene expression noise; a property that might be particularly beneficial for reliable functioning of the cell. The gene expression is inherently stochastic due to the probabilistic nature of various molecular interactions associated with gene expression [7, 8]. The stochasticity leads to random fluctuations in the protein levels although it is known that many biological functions of the cell require fine-tuning of necessary protein levels. In this regard, it has been found that sRNA mediated repression of gene expression leads to reduced fluctuations in the protein level as compared to transcription factor mediated repression [5]. Further, optimal noise buffering has also been seen in more complex genetic circuits such as incoherent sRNA mediated feed-forward loops (FFL) [9, 10], sRNA-driven feed-forward loop [11] etc., where dual strategies i.e. regulation at both transcriptional and translational levels are employed.

Recent studies have revealed a particularly subtle and complex strategy of miRNA mediated gene regulation wherein a given species of miRNA interacts with a number of different mRNA targets [12–16]. The primary goal

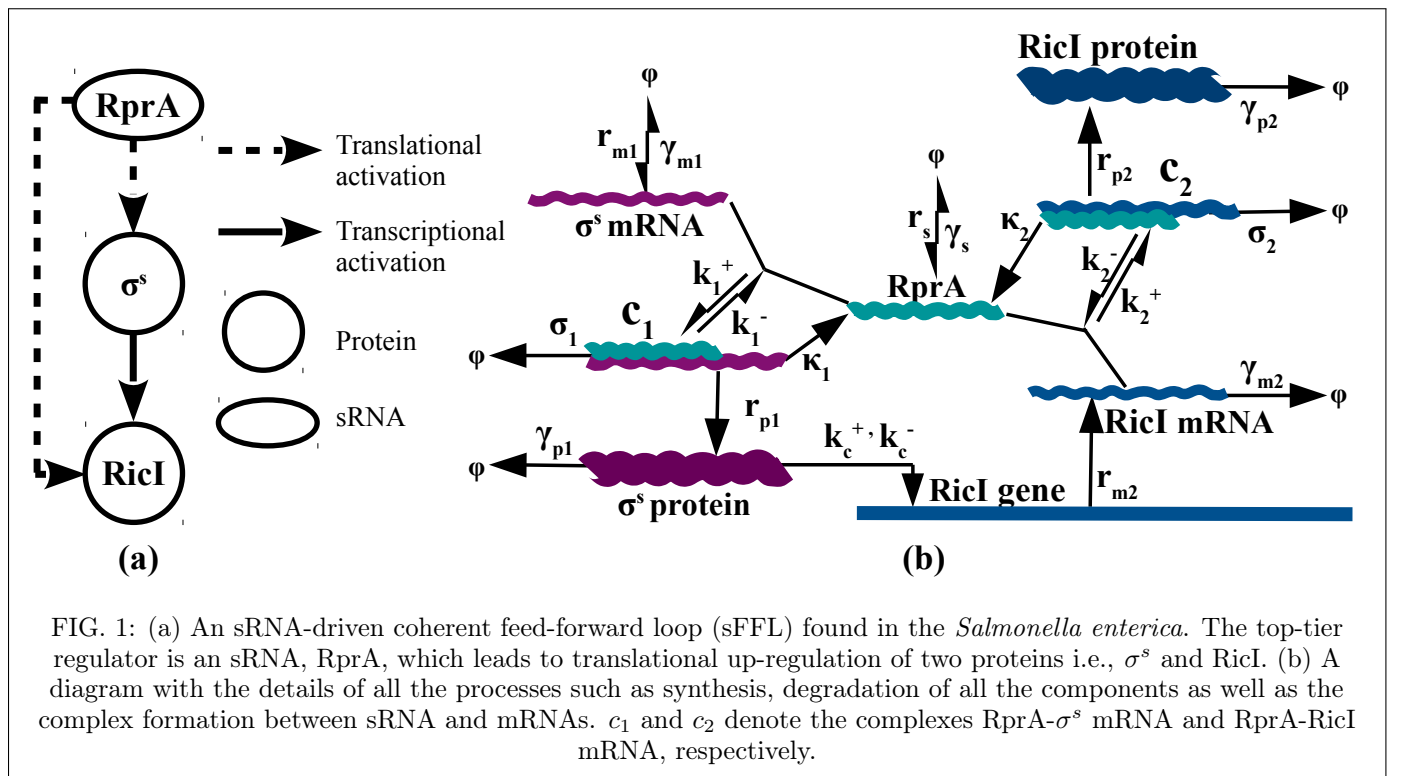
*Electronic address: ¹ swathi.rf0897@cftri.res.in

² sutapa@cftri.res.in

of such miRNA-mRNA network is to give rise to regulation through competition in which different mRNA targets compete for binding to the same miRNA species (also known as competing endogenous RNA or ceRNA effect). In other words, the miRNAs may function as a channel through which the change in concentration level in one type of target mRNA can be conveyed to another. It has been shown that such indirect miRNA mediated cross-talk may outperform direct regulation under certain circumstances [15]. Additionally, it has been found that such miRNA mediated cross-talk between mRNAs results in a broad impact on the protein level such as enhancing the stability of highly expressed proteins, altering the correlation patterns of coregulated interacting

proteins apart from, in general, fine-tuning the protein levels [16].

In the present paper, our attention is on a network motif where the sRNA mediated cross-talk between mRNAs seems to play an important role in regulating the target protein synthesis. Network motifs are specific sub-networks that have frequent recurrences in large regulatory networks as some of their major building blocks [17]. Such motifs usually have distinct functionalities and it is believed that such motifs are chosen evolutionarily due to distinct advantages they provide to the cell. The network motif of our interest is a feed-forward loop (FFL) which is driven by an sRNA (see figure 1(a)) unlike the commonly found FFLs driven by transcription factors [18].



We refer to this sRNA-driven FFL as sFFL in the following. In general, the top-tier regulator in FFL drives the target protein synthesis along two pathways; one pathway involves a direct regulation of the target protein synthesis and the other involves an indirect regulation via up- or down-regulation of an intermediate regulator of the target protein. For a purely transcriptional FFL, all the interactions are at the transcription level and the top-tier as well as the intermediate regulators are transcription factors. The sFFL introduced here is different from another kind of transcription factor driven FFLs which involve sRNA as an intermediate regulator of the target protein [10, 19, 20]. The feature that remains common

in all these FFLs is that the top-tier regulator regulates expression of two distinct genes. In the case of sFFL, an sRNA being the top-tier regulator, regulates the translational activities of two different mRNAs along two regulatory pathways of FFL and thus gives rise to distinct regulatory features through sRNA induced cross-talk between mRNAs.

The existence of such sFFL has been found experimentally very recently in the context of stress response of *Salmonella enterica* subjected to stress due to a bactericidal agent, bile salt [18]. In this sFFL, an sRNA, RprA, activates the synthesis of the target protein, RicI, directly through translational activation of RicI mRNA and in-

TABLE I: Mathematical notations for concentrations of various components of sFFL

Notations	Biological sFFL
s (sRNA)	RprA sRNA
m_1 (mRNA1)	σ^s -mRNA
c_1 (complex-1)	RprA- σ^s -mRNA complex
p_1 (protein-1)	σ^s protein
m_2 (mRNA2)	RicI-mRNA
c_2 (complex-2)	RprA-RicI-mRNA complex
p_2 (protein-2)	RicI protein

directly via translational activation in the synthesis of the alternative sigma-factor, σ^s , which transcriptionally activates RicI gene (see figure 1(a) and 1(b)). By base-pairing with the σ^s mRNA, RprA opens up the translation inhibitory loop in the 5' untranslated region (UTR) of σ^s -mRNA and facilitates ribosome binding to initiate translation leading to the synthesis of σ^s protein [21]. σ^s protein being a transcriptional activator of RicI gene leads to an enhanced synthesis of RicI-mRNA which are, then, translationally activated by sRNA, RprA, resulting in an up-regulation in RicI protein synthesis. Here again, RprA facilitates ribosome binding by opening up the translation inhibitory loop of RicI-mRNA. Such an FFL with activating regulation along both the paths is known as coherent FFL while an FFL involving opposing kind of regulation along the two paths is known as incoherent FFL. An up-regulation of RicI protein happens in response to the membrane damaging activity of the bile salt. As a response to the stress, the bacterial cell prefers to shut down the energy-expensive processes associated with horizontal gene transfer although horizontal gene transfer plays a significant role in bacteria's survival under normal conditions. By interfering with the formation of the pilus that is necessary for bacterial conjugation during horizontal gene transfer, RicI protein down-regulates the process of horizontal gene transfer and protects the bacteria from additional energy loss associated with this process [18]. For the rest of the paper, we follow general notations for various regulatory molecules as listed in table I.

The miRNA mediated cross-talk between different mRNAs is a subject of extensive investigations currently. Some of the earlier studies were based on simplified models involving different species of mRNA molecules that were co-repressed by a single miRNA species [13]. The effect of miRNA mediated cross-talk on the protein products of these mRNA targets and on the protein-protein interaction were also studied later starting with this basic framework [16]. In view of the earlier studies, sFFL considered here is somewhat special for the following reasons. Instead of sRNA mediated repression, which is the most common form of regulation by sRNAs, here the sRNA leads to translational activation of two different mRNAs. Further, the FFL not only involves sRNA mediated inter-

actions between the mRNAs, but it also involves a direct interaction between the mRNAs. The latter is due to the fact that an up-regulation of one species of mRNA (m_1 i.e. σ^s -mRNA) gives rise to enhanced transcription of the other species of mRNA (m_2 i.e. RicI-mRNA) via up-regulation of the protein product of m_1 (i.e. σ^s protein) [18]. Thus, the sFFL provides a unique platform to study how the combined effect of sRNA mediated cross-talk and a direct interaction between the mRNAs influence the target protein regulation.

Using various tools of mathematical modelling, we quantify the effect of sRNA mediated cross-talk on the target protein concentration. The cross-talk is seen by studying how the concentration of mRNA2 (m_2) and sRNA (s) change as the synthesis rate of mRNA1 (m_1) is changed. Following the table, we refer the mRNAs as well as their concentrations as m_1 and m_2 . The same convention is followed for the two species of proteins. As the concentration of m_1 increases, there is a reduction in the free sRNA concentration since m_1 molecules tend to form complexes with available free sRNAs and this, consequently, leads to an increase in the concentration of free m_2 molecules since sRNAs are largely bound to m_1 . Interestingly, the change in the concentrations shows a sensitive (or susceptible) region over a narrow range of m_1 synthesis rate (r_{m_1}) where, with a small increase in r_{m_1} , there is an abrupt change in various concentrations. The major findings of this study are as follows. (1) The sRNA mediated cross-talk leads to an initial increase in the target protein concentration with the synthesis rate, r_{m_1} . With further increase in r_{m_1} , the target protein concentration reaches a peak and then undergoes a sharp decrease. Hence, it appears that the network motif is designed to perform most efficiently when the supply of m_1 (i.e. σ^s -mRNA for this sFFL) is low. Since σ^s is a key stress response regulator responsible for various other regulatory activities, this might be an efficient method for maximum utilisation of available σ^s -mRNA. (2) The sRNA mediated cross-talk plays a more important role in regulating the target protein concentration compared to the direct interaction between m_1 and m_2 . (3) We show that the range of r_{m_1} over which the maximum synthesis of the target protein takes place also corresponds to the range where the noise in the target protein concentration is minimal. This result is further supported by stochastic simulations based on Gillespie algorithm. Overall, the present work suggests that the sRNA mediated cross-talk not only ensures maximum target protein synthesis with an efficient use of σ^s -mRNA, it also contributes to maximal noise attenuation in the target protein concentration during its synthesis.

II. RESULTS

A. Model and steady-state results

In the following, we present a model for the sFFL describing how the concentrations of various regulatory components change with time. The equations that we use for our calculations are

$$\dot{s} = r_s - \gamma_s s - k_1^+ s m_1 - k_2^+ s m_2 + (k_1^- + \kappa_1)c_1 + (k_2^- + \kappa_2)c_2, \quad (1)$$

$$\dot{m}_1 = r_{m_1} - \gamma_{m_1} m_1 - k_1^+ s m_1 + k_1^- c_1, \quad (2)$$

$$\dot{c}_1 = k_1^+ s m_1 - (k_1^- + \sigma_1 + \kappa_1)c_1, \quad (3)$$

$$\dot{p}_1 = r_{p_1} c_1 - \gamma_{p_1} p_1, \quad (4)$$

$$\dot{m}_2 = \frac{r_{m_2} k_c p_1}{1 + k_c p_1} - \gamma_{m_2} m_2 - k_2^+ s m_2 + k_2^- c_2, \quad (5)$$

$$\dot{c}_2 = k_2^+ s m_2 - (k_2^- + \sigma_2 + \kappa_2)c_2, \quad (6)$$

$$\dot{p}_2 = r_{p_2} c_2 - \gamma_{p_2} p_2, \quad (7)$$

where, in general, $\dot{x} = \frac{d}{dt}x$. Here, we have used general notations for various concentrations as listed in table I. The rate parameters r and γ represent synthesis and degradation rates in general. c_1 and c_2 represent sRNA-mRNA complexes of two different kinds. k^+ and k^- represent the association and dissociation rates of these complexes. κ and σ represent catalytic and stoichiometric degradation rates of the complexes, respectively. While sRNAs are reused upon catalytic degradation, in the case of stoichiometric degradation the complex is degraded completely.

In the steady-state, the solutions for m_1 , m_2 and s are

$$m_1 = m_1^* F_1(s), \quad m_2 = \frac{m_2^* k_c a s F_1(s) F_2(s)}{1 + k_c a s F_1(s)}, \quad \text{where} \quad (8)$$

$$F_1(s) = \frac{1}{1 + s/s_{01}} \quad \text{with} \quad s_{01} = \frac{\gamma_{m_1} k_1^- + \sigma_1 + \kappa_1}{k_1^+}, \quad (9)$$

$$F_2(s) = \frac{1}{1 + s/s_{02}} \quad \text{with} \quad s_{02} = \frac{\gamma_{m_2} k_2^- + \sigma_2 + \kappa_2}{k_2^+}, \quad (10)$$

$$m_1^* = \frac{r_{m_1}}{\gamma_{m_1}}, \quad m_2^* = \frac{r_{m_2}}{\gamma_{m_2}}, \quad a = \frac{r_{p_1}}{\gamma_{p_1}} \frac{k_1^+ m_1^*}{(k_1^- + \sigma_1 + \kappa_1)}. \quad (11)$$

The steady-state concentration of sRNA can be found upon solving the following algebraic equation for s

$$r_s - \gamma_s s - r_{m_1} \zeta_1 s F_1(s) - r_{m_2} \zeta_2 \frac{k_c a s^2 F_1(s) F_2(s)}{1 + k_c a s F_1(s)} = 0, \quad (12)$$

$$\text{with } \zeta_1 = \frac{k_1^+ \sigma_1}{\gamma_{m_1} (k_1^- + \sigma_1 + \kappa_1)}, \quad \zeta_2 = \frac{k_2^+ \sigma_2}{\gamma_{m_2} (k_2^- + \sigma_2 + \kappa_2)}. \quad (13)$$

Figure 2 shows how sRNA and mRNA concentrations change as r_{m_1} , the transcription rate of m_1 , is changed.

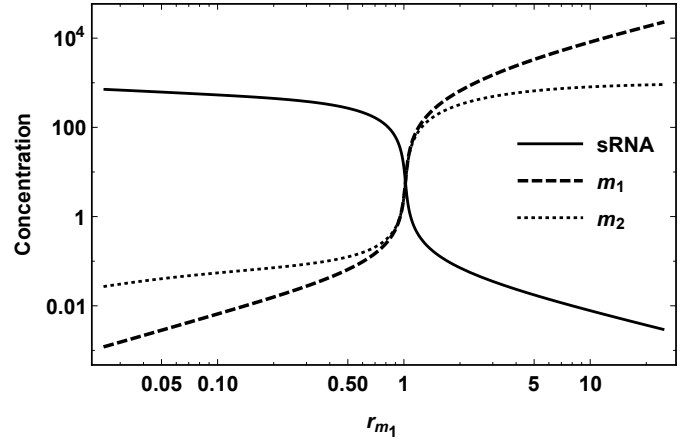


FIG. 2: Changes in various concentrations with r_{m_1} .

The parameter values used for these plots are:

$r_s = r_{m_2} = 1$, $k_1^+ = k_2^+ = 0.1$, $k_1^- = k_2^- = 0.05$, $\sigma_1 = \sigma_2 = \kappa_1 = \kappa_2 = 0.01$ and $k_c = 0.1$. Degradation rates of sRNA, mRNA m_1 and m_2 , proteins p_1 and p_2 are 0.001 and the synthesis rates of p_1 and p_2 are 0.01.

The presence of sRNA induced effective interaction between m_1 and m_2 is apparent here since a change in the transcription rate of m_1 affects the equilibrium concentrations of the sRNA and m_2 . Intuitively, as the concentration of m_1 increases, these mRNAs bind the sRNAs causing a reduction in the concentration of free sRNAs and, as a consequence, an increase in the concentration of free m_2 . Interestingly, figure 2 shows that, over a narrow range of r_{m_1} , there exists a sensitive region where the concentrations of s , m_1 and m_2 change sharply as r_{m_1} is changed. We shall show in the following that over this region, the sFFL attenuates the fluctuations (noise) in the target protein concentration maximally. In sFFL, there is a direct interaction between mRNAs, m_1 , and m_2 , since the protein product of m_1 is a transcriptional activator of p_2 . The change in the concentration of m_2 with r_{m_1} is, thus, expected. However, as we show below, a large contribution in the increase of m_2 concentration comes from the sRNA induced cross-talk between mRNAs.

B. Response functions

In order to quantify the interactions among various regulatory molecules, we introduce the following response functions

$$\chi_{ij} = \frac{\partial m_i}{\partial r_{m_j}}, \quad \text{where } i, j = 1, 2 \quad \text{with } i \neq j \quad (14)$$

$$\chi_{si} = \frac{\partial s}{\partial r_{m_i}}, \quad \text{where } i = 1, 2. \quad (15)$$

Here χ_{ij} represents the response in terms of a change in the concentration of a specific kind of mRNA (m_1 or m_2)

as the transcription rate of the other mRNA is changed. In similar way, χ_{si} represents the change in sRNA concentration as the transcription rates of the i th mRNA,

i.e. r_{m_1} or r_{m_2} is changed.

Using (8) and (12) we find the response functions as

$$\chi_{12} = m_1^* F_1' \chi_{s2}, \quad \chi_{21} = \frac{m_2^* k_c a}{(1 + k_c a s F_1)^2} \left\{ \chi_{s1} [F_1 F_2 + s(F_1' F_2 + F_1 F_2')] + k_c a s^2 F_1^2 F_2' \right\} + \frac{s F_2 F_1}{r_{m_1}} \quad \text{with (16)}$$

$$\chi_{s1} = \frac{-\zeta_1 s F_1 - \zeta_2 r_{m_2} k_c a s^2 F_2 F_1 [r_{m_1} (1 + k_c a s F_1)^2]^{-1}}{\gamma_s + r_{m_1} \zeta_1 [F_1 + s F_1'] + \frac{r_{m_2} \zeta_2 k_c a s}{(1 + k_c a s F_1)^2} [2 F_1 F_2 + s(F_1' F_2 + F_1 F_2') + k_c a s F_1^2 (F_2 + s F_2')]} \quad \text{and (17)}$$

$$\chi_{s2} = \frac{-\zeta_2 k_c a s^2 F_2 F_1 [(1 + k_c a s F_1)]^{-1}}{\gamma_s + r_{m_1} \zeta_1 [F_1 + s F_1'] + \frac{r_{m_2} \zeta_2 k_c a s}{(1 + k_c a s F_1)^2} [2 F_1 F_2 + s(F_1' F_2 + F_1 F_2') + k_c a s F_1^2 (F_2 + s F_2')]} \quad (18)$$

where $F_1' = \frac{\partial}{\partial s} F_1$ and $F_2' = \frac{\partial}{\partial s} F_2$. The response in the sRNA concentration is always negative ($\frac{\partial s}{\partial r_{m_1}} < 0$, $\frac{\partial s}{\partial r_{m_2}} < 0$) indicating that the concentration of free sRNA decreases with enhanced synthesis of mRNAs, m_1 and m_2 . Such reduction in free sRNA happens due to the sRNA-mRNA complex formation. The response function χ_{21} has two parts. The first term indicates a change in m_2 as a result of the change in free sRNA concentration. This happens due to an enhanced sRNA-mRNA1 complex (c_1) formation as the transcription rate of mRNA m_1 is increased. This indirect influence of the transcription rate of m_1 on m_2 concentration via sRNA is a signature of sRNA induced cross-talk between the mRNAs. The second term in the equation for χ_{21} (see equation 16) originates from the direct interaction between m_1 and m_2 because of the transcriptional activation of m_2 by the protein product of m_1 . From the equation for χ_{12} it is clear that the synthesis rate of m_2 affects the concentration of m_1 only through an indirect interaction mediated by sRNA. Further, as observed earlier [13], in the absence of stoichiometric complex decay (i.e. for $\sigma_1 = \sigma_2 = 0$), the indirect interaction term disappears since, in this case, $\frac{\partial s}{\partial r_{m_1}} = 0$ and $\frac{\partial s}{\partial r_{m_2}} = 0$. The response functions can be compared with sRNA-driven cascade network (sCN) where sRNA post-transcriptionally up-regulates p_1 synthesis and p_1 transcriptionally up-regulates p_2 synthesis. (see appendix A for details). Thus unlike sFFL, in sCN, there is no competition for sRNA sharing. Consequently, the response functions, in this case, are (see appendix A for details)

$$\chi_{12} = 0, \quad \chi_{21} = \frac{k_c m_2^* a}{(1 + k_c a s F_1)^2} \left\{ \chi_{s1} [F_1 + s F_1'] + \frac{s F_1}{r_{m_1}} \right\} \quad (19)$$

$$\text{with } \chi_{s1} = \frac{-\zeta_1 s F_1}{\gamma_s + r_{m_1} \zeta_1 [F_1 + s F_1']} \quad \text{and } \chi_{s2} = 0 \quad (20)$$

The vanishing of χ_{12} is expected as, in contrary to sFFL, here the increase in m_2 synthesis does not affect the

sRNA concentration.

In order to see how the response function χ_{21} changes with r_{m_1} , we have obtained χ_{21} numerically using equations (8) and (12). For an estimate of the contribution from the direct interaction part (the second term in χ_{21} of equation (16)), χ_{21d} , we have plotted $\chi_{21d} = m_2^* \frac{k_c a s F_1 F_2}{r_{m_1} (1 + k_c a s F_1)^2}$ after substituting the solution for s as a function of r_{m_1} . Figure 3(a) shows the rate of change of concentration of m_2 with respect to r_{m_1} (i.e. χ_{21})

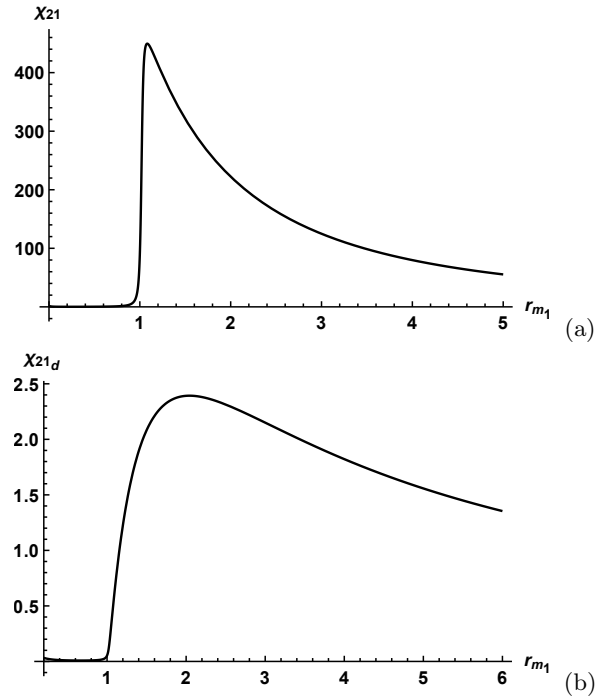


FIG. 3: (a) The response function, χ_{21} for sFFL plotted with r_{m_1} , the transcription rate of mRNA, m_1 . (b) The response due to the transcriptional interaction between p_1 (the protein product of m_1) and m_2 . Same parameter values as in figure 2 are used here.

for different values of r_{m_1} . The presence of the sensitive region, as discussed before, appears very prominently in these figures. As figures 3(a) and 3(b) indicate, the contribution of the direct interaction part to χ_{21} , in general, is quite small compared to the sRNA-mediated part.

C. Effect of sRNA mediated cross-talk on the target protein concentration

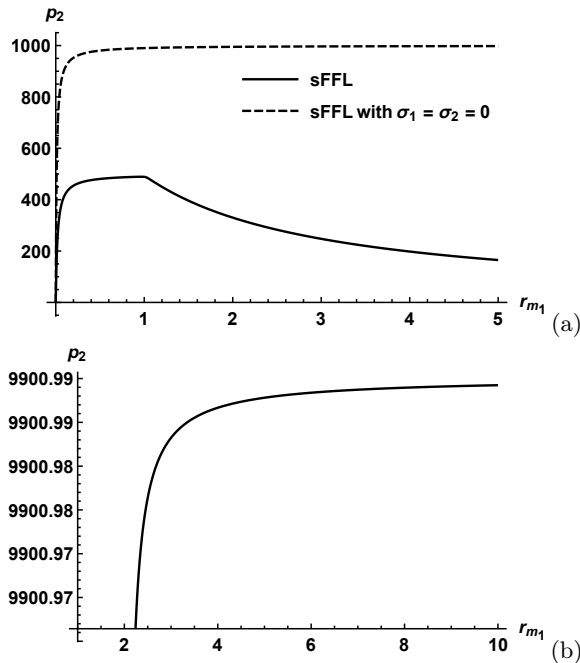


FIG. 4: Variation of target protein expression with the transcription rate (r_{m_1}) of mRNA, m_1 for (a) sFFL with and without cross-talk ($\sigma_1 = \sigma_2 = 0$) and for (b) sRNA-driven cascade network (sCN). Parameter values are as same as those chosen for figure 2.

In this section, we focus on the influence of sRNA mediated cross-talk between mRNAs on the target protein concentration. When there is complete recycling of sRNA (i.e. $\sigma_1 = \sigma_2 = 0$), there is no sRNA mediated cross-talk between the mRNAs since $\chi_{s1} = \chi_{s2} = 0$. Under such conditions, the target protein concentration increases initially with the transcription rate, r_{m_1} , and saturates eventually as a consequence of the saturation kinetics associated with transcriptional activation in m_2 synthesis by p_1 (see figure 4(a)). In the presence of sRNA induced cross-talk (i.e. $\sigma_1, \sigma_2 \neq 0$), with the increase in r_{m_1} , the target protein concentration goes through a peak followed by a sharp decrease. This happens near the sensitive region where the concentration of free sRNA available for translational activation of p_2 drops down drastically. In the case of sCN (see figure 4(b)), the protein concentration reaches a saturation value which persists

over the entire range. Thus it appears that as far as the target protein concentration is concerned, the network performs most efficiently for low concentration of σ^s mRNA. This feature may be beneficial for the cell since σ^s is a key regulator associated with different types of stress-response of the cell.

D. Noise Analysis

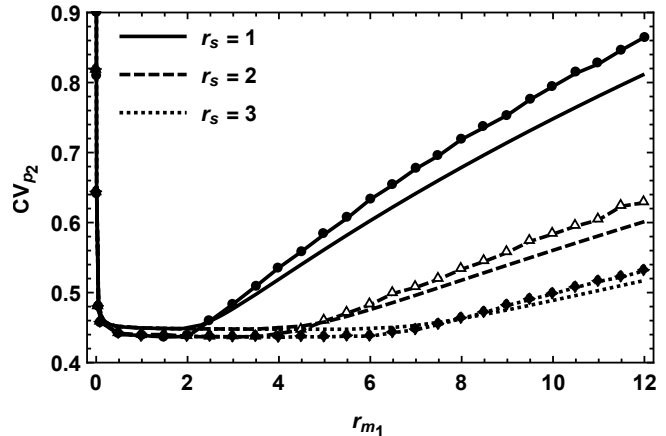


FIG. 5: The coefficient of variation for the target protein in sFFL as a function of r_{m_1} , the synthesis rate of the intermediate mRNA, m_1 , for different values of sRNA synthesis rate, r_s . The coefficient of variation is obtained by finding numerical solutions for necessary moments using Mathematica (lines without markers).

The parameter values used for this are

$$\begin{aligned} \gamma_s = \gamma_{m_1} = \gamma_{m_2} = \gamma_{p_1} = \gamma_{p_2} = 0.001, \\ r_{m_2} = r_{p_1} = r_{p_2} = 0.01, k_1^+ = k_2^+ = 0.1, \\ k_1^- = k_2^- = 0.05, k_c = 0.1 \text{ and} \end{aligned}$$

$\kappa_1 = \kappa_2 = \sigma_1 = \sigma_2 = 0.005$. The lines with markers represent the same found from stochastic simulations based on the Gillespie algorithm. The details regarding the reactions and the reaction rates are presented in appendix D.

The aim of the present section is to find how the sRNA induced cross-talk influences the noise buffering characteristics of sFFL. We begin with the master equation that describes how the probability of a given state changes with time [22]. A state of this system is described by the numbers of sRNA, two different mRNAs and two different protein molecules. The state of the system changes as the numbers of various molecules change due to possible reactions taking place at given rates. We introduce $P_{s,m_1,p_1,m_2,p_2}(t)$ as the probability at time t that the system is in a state in which the number of sRNA, mRNA and protein molecules are s , m_1 , m_2 , p_1 and p_2 , respectively. The master equation describing the rate of change of the probability function with time can be written as

$$\begin{aligned}
\partial_t P_{s,m_1,p_1,m_2,p_2}(t) = & r_s (P_{s-1,m_1,p_1,m_2,p_2} - P_{s,m_1,p_1,m_2,p_2}) + \gamma_s ((s+1)P_{s+1,m_1,p_1,m_2,p_2} - sP_{s,m_1,p_1,m_2,p_2}) \\
& + r_{m_1} (P_{s,m_1-1,p_1,m_2,p_2} - P_{s,m_1,p_1,m_2,p_2}) + \gamma_{m_1} ((m_1+1)P_{s,m_1+1,p_1,m_2,p_2} - m_1P_{s,m_1,p_1,m_2,p_2}) \\
& + r'_{p_1} s m_1 (P_{s,m_1,p_1-1,m_2,p_2} - P_{s,m_1,p_1,m_2,p_2}) + \gamma_{p_1} ((p_1+1)P_{s,m_1,p_1+1,m_2,p_2} - p_1P_{s,m_1,p_1,m_2,p_2}) \\
& + r_{m_2} (p_1) (P_{s,m_1,p_1,m_2-1,p_2} - P_{s,m_1,p_1,m_2,p_2}) + \gamma_{m_2} ((m_2+1)P_{s,m_1,p_1,m_2+1,p_2} - m_2P_{s,m_1,p_1,m_2,p_2}) \\
& + r'_{p_2} s m_2 (P_{s,m_1,p_1,m_2,p_2-1} - P_{s,m_1,p_1,m_2,p_2}) + \gamma_{p_2} ((p_2+1)P_{s,m_1,p_1,m_2,p_2+1} - p_2P_{s,m_1,p_1,m_2,p_2}) \\
& + g_1 ((s+1)(m_1+1)P_{s+1,m_1+1,p_1,m_2,p_2} - s m_1 P_{s,m_1,p_1,m_2,p_2}) + d_1 s ((m_1+1)P_{s,m_1+1,p_1,m_2,p_2} - m_1 P_{s,m_1,p_1,m_2,p_2}) \\
& + g_2 ((s+1)(m_2+1)P_{s+1,m_1,p_1,m_2+1,p_2} - s m_2 P_{s,m_1,p_1,m_2,p_2}) + d_2 s ((m_2+1)P_{s,m_1,p_1,m_2+1,p_2} - m_2 P_{s,m_1,p_1,m_2,p_2}).
\end{aligned} \tag{21}$$

Here $\partial_t P_{s,m_1,p_1,m_2,p_2}(t) = \frac{\partial}{\partial t} P_{s,m_1,p_1,m_2,p_2}(t)$. Various terms on the right hand side of the equation account for different reactions representing synthesis and degradation of various molecules (see appendix B for details). Here

$$\begin{aligned}
r'_{p_1} = \frac{r_{p_1} k_1^+}{k_1^- + \sigma_1 + \kappa_1}, \quad r'_{p_2} = \frac{r_{p_2} k_2^+}{k_2^- + \sigma_2 + \kappa_2}, \quad g_1 = \frac{k_1^+ \sigma_1}{k_1^- + \sigma_1 + \kappa_1}, \quad g_2 = \frac{k_2^+ \sigma_2}{k_2^- + \sigma_2 + \kappa_2} \quad d_1 = \frac{k_1^+ \kappa_1}{k_1^- + \sigma_1 + \kappa_1}, \\
\text{and } d_2 = \frac{k_2^+ \kappa_2}{k_2^- + \sigma_2 + \kappa_2}.
\end{aligned} \tag{22}$$

The transcriptional activation of p_2 by p_1 is taken into account by the Hill function, $r_{m_2}(p_1) = \frac{r_{m_2} k_c p_1}{1 + k_c p_1}$. For the present calculation, the Hill function is approximated about the average steady-state density $\langle p_1 \rangle$ as

$$r_{m_2}(p_1) = r_{m_2}^0 + r_{m_2}^1 p_1 \quad \text{where} \quad r_{m_2}^0 = \frac{r_{m_2} k_c^2 \langle p_1 \rangle^2}{(1 + k_c \langle p_1 \rangle)^2} \quad \text{and} \quad r_{m_2}^1 = \frac{r_{m_2} k_c}{(1 + k_c \langle p_1 \rangle)^2}. \tag{23}$$

Next, we consider the moment generating function

$$G(z_1, z_2, z_3, z_4, z_5) = \sum_{s,m_1,p_1,m_2,p_2} z_1^s z_2^{m_1} z_3^{p_1} z_4^{m_2} z_5^{p_2} P_{s,m_1,p_1,m_2,p_2} \tag{24}$$

whose time evolution is described as

$$\begin{aligned}
\partial_t G = & r_s (z_1 - 1)G + \gamma_s (1 - z_1) \partial_{z_1} G + r_{m_1} (z_2 - 1)G + \gamma_{m_1} (1 - z_2) \partial_{z_2} G + r'_{p_1} z_1 z_2 (z_3 - 1) \partial_{z_1 z_2}^2 G + \gamma_{p_1} (1 - z_3) \partial_{z_3} G \\
& + r_{m_2}^0 (z_4 - 1)G + r_{m_2}^1 z_3 (z_4 - 1) \partial_{z_3} G + \gamma_{m_2} (1 - z_4) \partial_{z_4} G + r'_{p_2} z_1 z_4 (z_5 - 1) \partial_{z_1 z_4}^2 G + \gamma_{p_2} (1 - z_5) \partial_{z_5} G \\
& + g_1 (1 - z_1 z_2) \partial_{z_1 z_2}^2 G + g_2 (1 - z_1 z_4) \partial_{z_1 z_4}^2 G + d_1 z_1 (1 - z_2) \partial_{z_1 z_2}^2 G + d_2 z_1 (1 - z_4) \partial_{z_1 z_4}^2 G,
\end{aligned} \tag{25}$$

where $\partial_{z_i} G = \frac{\partial}{\partial z_i} G$ and $\partial_{z_i z_j}^2 G = \frac{\partial^2}{\partial z_i \partial z_j} G$.

In the steady state ($\partial_t G = 0$), the right hand side of equation (25) is equated to zero. Various average quantities (moments) can be calculated by differentiating the resulting steady-state equation with respect to appropriate z_i and then considering $z_i = 1$ for all i . The first moments follow from G as $G_1 = \langle s \rangle$, $G_2 = \langle m_1 \rangle$, $G_3 = \langle p_1 \rangle$ etc. where $G_i = \partial_{z_i} G |_{\{z_i\}=1}$ with $\{z_i\} = 1$ indicating $z_i = 1$ for all i . The second moments similarly can be determined from G_{ij} where $G_{ij} = \partial_{z_i z_j}^2 G |_{\{z_i\}=1}$. We are in particular interested in the target protein fluctuation which can be measured through the coefficient of variation, $CV_{p_2} = (G_{55} + G_5 - G_5^2)^{1/2} / G_5$. The derivation of the moments G_5 and G_{55} appears to be complex since the evaluation of a moment of a given order involves

evaluation of various higher order moments. In order to simplify the derivation, we restrict ourselves up to second moments and express the third moments necessary for this derivation in terms of lower order moments using Gaussian approximation [23]. The results for moments up to second order and the approximate forms of the required third order moments are presented in appendix B2.

Moments required for the evaluation of the coefficient of variation are found numerically using Mathematica. The coefficient of variation as a function of r_{m_1} for different values of, r_s , the sRNA synthesis rate, is shown in figure 5. It is clear that the fluctuations in the target protein concentration are minimum over a range of r_{m_1} .

Interestingly, this minimum region overlaps with the sensitive region shown in figure 2. As r_s increases, the sensitive region extends towards larger r_{m_1} . Figure 5 shows that the minimum fluctuation region also changes accordingly and there is a systematic increase in the fluctuation beyond this region. In order to see the role of cross-talk in noise processing characteristics, we have also obtained the coefficient of variation for the target protein number for sFFL with $\sigma_1 = \sigma_2 = 0$ (no cross-talk) and sCN (see appendix B and C). The coefficients of variation plotted with r_{m_1} indicate the absence of optimal noise attenuation.

In order to verify the above observations, we obtain exact results for the coefficient of variation of the target protein number from stochastic simulations based on Gillespie algorithm [24, 25]. In simulations, we begin with an initial number of various molecular species. The key reactions in our simulation include synthesis, degradation, complex association/dissociation and transcriptional interactions between the DNA and the transcription factor. In stochastic simulations, an event or a reaction and the interval between two successive reactions are chosen probabilistically. Based on the reaction that takes place, at each simulation step, the number of molecular species is updated accordingly. We allow the system to evolve for 5×10^7 steps and record the target protein number after every 500 steps leaving about initial 2×10^5 steps. The coefficient of variation averaged over 100 samples has been presented in figure 5. A remarkable agreement between results from simulations and from generating function method further confirms that maximum noise attenuation in the target protein level happens over the sensitive region.

Our conclusions on how the target protein concentration as well as its fluctuations around the mean value change with r_{m_1} can be summarized through a single plot shown in figure 6. This plot clearly shows that the range of r_{m_1} over which the target protein concentration reaches its maximum also corresponds to the range of maximum noise attenuation in the target protein level. Thus it appears that sRNA-mediated cross-talk plays a subtle role in ensuring that maximal target protein synthesis happens with the least noise in the target protein level.

III. DISCUSSION

Small noncoding RNAs in bacterial cells are major regulators driving a number of biological processes such as stress response, biofilm formation, quorum sensing etc. under different kinds of environmental signals. It is commonly found that one species of sRNA can regulate translation of several species of mRNAs and also a species of mRNA can be targeted by more than one species of sRNAs. The complex network formed thereby is believed to be able to integrate different types of environmental signals in a unified manner. The regula-

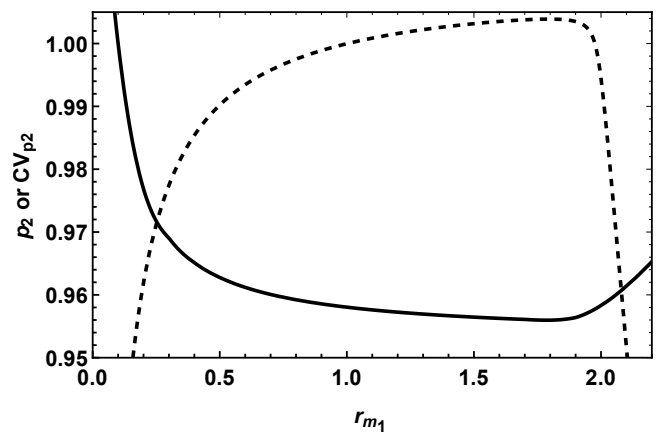


FIG. 6: Target protein concentration (dashed line) (normalized with respect to its peak value) and the coefficient of variation (solid line) plotted with r_{m_1} . The coefficient of variation is obtained from the analysis based on generating functions. The parameter values are same as those used for figure 5. For this figure $r_s = 1$.

tion here primarily happens through sharing of sRNAs by several co-regulated mRNA targets. If the concentration of one species of mRNA, say m_1 increases, the sRNAs are expected to bind to m_1 predominantly due to its increased concentration. This leads to an increase in sRNA-mRNA1 complex (c_1) concentration and consequently a lowering of available free sRNAs and an increase in the concentration of other mRNA targets. The sharing of sRNA thus provides a link between its target mRNAs leading to an sRNA mediated effective interaction (cross-talk) between the mRNAs. Mostly this link extends over mRNAs from different networks and the regulation through sRNA sharing may give rise to the possibility of integrating biological processes governed by different networks. In the present work, we are interested in understanding the effect of sRNA mediated cross-talk between two species of mRNAs in a network motif comprised of feed-forward loop driven by an sRNA. Thus unlike earlier work, our focus is on the effect of sRNA sharing on the target protein synthesis in a network motif.

In the feed-forward loop of our interest, the top-tier regulator is an sRNA (RprA) that regulates the target protein (RicI) synthesis along two pathways. While one pathway involves a direct translational activation of RicI protein by RprA, the other pathway involves an indirect activation of RicI expression via translational activation of its transcriptional activator (σ^s) by RprA. The sRNA thus translationally activates its two target mRNAs, RicI mRNA and σ^s mRNA. Such an sRNA-driven feed-forward loop (sFFL) is found to play a significant role in regulating horizontal gene transfer in *Salmonella enterica* when the bacteria is subjected to stress due to membrane damaging activities of a bactericidal agent,

bile salt. Since horizontal gene transfer is an energy-expensive process, inhibiting such processes during stress conditions might be a preferred strategy for additional protection of the bacteria. RicI protein participates in the stress-response activity by interfering with pilus formation which is necessary for bacterial conjugation during the process of horizontal gene transfer.

The σ^s protein which is a transcriptional activator of RicI is known to be a key stress-response regulator that responds to various other environmental stress conditions too. The up-regulation of σ^s protein, however, does not necessarily imply an up-regulation of RicI protein. The design of sFFL ensures that RicI is up-regulated by combined action along both the paths of sFFL. The present analysis further shows that as a result of sRNA-mediated cross-talk, the network also performs most efficiently when the σ^s mRNA concentration is low. This result is concluded from the following observations. If the synthesis rate of σ^s mRNA is increased, the concentration of free sRNA decreases as a consequence of sRNA-mRNA1 complex formation. Due to reduced availability of free sRNA molecules for binding, the level of free m_2 increases. This effect of cross-talk linking the two species of mRNAs is more abrupt over a narrow range of m_1 synthesis rate which we refer as a sensitive region. In this region, a small increase in the synthesis rate gives rise to a sharp drop in the sRNA concentration along with a steep rise in the concentrations of the two mRNAs. As far as the target protein is concerned, it is found that with the increase in m_1 synthesis rate, the target protein concentration reaches a maximum and then decreases sharply as a consequence of a sharp drop in free sRNA in the sensitive region. Although a large number of m_2 are synthesized, the translation is less probable due to less availability of free sRNA molecules near the centre of the sensitive region. Such variation in the target protein concentration indicates that the motif performs most efficiently for low σ^s synthesis rate. Since σ^s is a major stress-response regulator associated with different kinds of environmental stress, such optimal utilization of σ^s mRNA might be a beneficial regulation strategy for the cell.

The gene expression is intrinsically noisy with noise originating from the randomness associated with various molecular interactions. This raises a fundamental question as to how cells perform in a robust manner despite significant variations in the gene expression levels. Recent evidences suggest that the architecture of the regulatory network determines the effect of gene expression noise on the target protein level, with some architecture leading to noise filtering, some leading to noise amplification etc. It is believed that the network motifs are evolutionarily selected based on the network architecture that may lead to such distinct noise processing characteristics. In view of this knowledge, we attempt to find the interplay of cross-talk and gene-expression noise in sFFL and its implications on fluctuations in the target protein level. To this end, we use a generating function based method

to obtain the coefficient of variation in the target protein level. Plotting the coefficient of variation with σ^s mRNA synthesis rate, we find that the noise in the target protein level is minimized over the sensitive region. In particular, the range over which maximum noise buffering happens also coincides with the range over which maximum target protein synthesis can be achieved. These results are verified through stochastic simulations based on Gillespie algorithm. Thus, it appears that the network architecture not only leads to maximum target protein synthesis under limited σ^s mRNA concentration, it also leads to maximal noise buffering while synthesizing the target protein to its maximum level. All these features resulting primarily from the sRNA mediated cross-talk between mRNAs indicate a complex and precise level of gene regulation through sRNA.

Conflict of interest: Authors declare no conflict of interest.

Acknowledgment: ST and SM thank DBT, India for financial support through grant no. BT/PR16861/BRB/10/1475/2016. ST thanks University Grants Commission (UGC), India for financial support under CSIR-UGC NET-JRF.

APPENDIX

Appendix A: sRNA-driven Cascade Network (sCN)

In this section, we consider the sRNA-driven cascade network (sCN) where sRNA translationally activates protein p_1 which then transcriptionally activates protein p_2 (see figure 7(b)). Thus, it is a cascade network where no sharing of free sRNA takes place. The variation in concentrations of various components of sCN with time is as follows,

$$\dot{s} = r_s - \gamma_s s - k_1^+ s m_1 + (k_1^- + \kappa_1) c_1, \quad (\text{A1})$$

$$\dot{m}_1 = r_{m_1} - \gamma_{m_1} m_1 - k_1^+ s m_1 + k_1^- c_1, \quad (\text{A2})$$

$$\dot{c}_1 = k_1^+ m_1 s - (k_1^- + \sigma_1 + \kappa_1) c_1, \quad (\text{A3})$$

$$\dot{p}_1 = r_{p_1} c_1 - \gamma_{p_1} p_1, \quad (\text{A4})$$

$$\dot{m}_2 = \frac{r_{m_2} k_c p_1}{1 + k_c p_1} - \gamma_{m_2} m_2, \quad \text{and} \quad (\text{A5})$$

$$\dot{p}_2 = r_{p_2} m_2 - \gamma_{p_2} p_2. \quad (\text{A6})$$

The steady-state concentrations of mRNAs m_1 and m_2 in terms of functions $F_1(s)$ and $F_2(s)$ are

$$m_1 = m_1^* F_1(s), \quad (\text{A7})$$

$$m_2 = \frac{m_2^* k_c a s F_1(s)}{1 + k_c a s F_1(s)} \quad \text{where} \quad (\text{A8})$$

$$m_1^* = \frac{r_{m_1}}{\gamma_{m_1}}, \quad m_2^* = \frac{r_{m_2}}{\gamma_{m_2}}, \quad a = \frac{r_{p_1} k_1^+ m_1^*}{\gamma_{p_1} (k_1^- + \sigma_1 + \kappa_1)}, \quad F_1(s) = \frac{1}{1 + s/s_{01}} \quad \text{and} \quad s_{01} = \frac{\gamma_{m_1} k_1^- + \sigma_1 + \kappa_1}{k_1^+}. \quad \text{In the steady-state,}$$

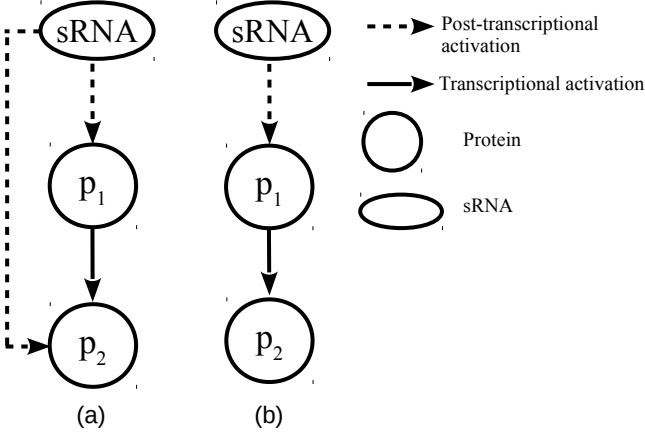


FIG. 7: Schematic diagrams for (a) sFFL and (b) sCN

the concentration of sRNA, can be found by solving $r_s - \gamma_s s - r_{m_1} \zeta_1 s F_1(s) = 0$, where $\zeta_1 = \frac{k_1^+ \sigma_1}{\gamma_{m_1} (k_1^- + \sigma_1 + \kappa_1)}$. The target protein concentration for sCN is $p_2 = \frac{r_{p_2}}{\gamma_{p_2}} m_2$ where m_2 is as shown in equation (A8).

Appendix B: Noise analysis for sFFL

1. Equations and notations

The reactions incorporated into the master equation, equation (21), are based on the following effective equations.

$$\dot{s} = r_s - \gamma_s s - g_1 s m_1 - g_2 s m_2, \quad (\text{B1})$$

$$\dot{m}_1 = r_{m_1} - \gamma_{m_1} m_1 - d_1 s m_1 - g_1 s m_1, \quad (\text{B2})$$

$$\dot{p}_1 = r'_{p_1} s m_1 - \gamma_{p_1} p_1, \quad (\text{B3})$$

$$\dot{m}_2 = \frac{r_{m_2} k_c p_1}{1 + k_c p_1} - \gamma_{m_2} m_2 - d_2 s m_2 - g_2 s m_2, \quad (\text{B4})$$

$$\text{and } \dot{p}_2 = r'_{p_2} s m_2 - \gamma_{p_2} p_2. \quad (\text{B5})$$

These equations are derived from (2)-(7) by substituting $c_1 = \frac{k_1^+ s m_1}{k_1^- + \sigma_1 + \kappa_1}$ and $c_2 = \frac{k_2^+ s m_1}{k_2^- + \sigma_2 + \kappa_2}$. While $g_1 = \frac{k_1^+ \sigma_1}{k_1^- + \sigma_1 + \kappa_1}$ and $g_2 = \frac{k_2^+ \sigma_2}{k_2^- + \sigma_2 + \kappa_2}$ correspond to combined degradation of sRNA and mRNA, $d_1 = \frac{k_1^+ \kappa_1}{k_1^- + \sigma_1 + \kappa_1}$ and $d_2 = \frac{k_2^+ \kappa_2}{k_2^- + \sigma_2 + \kappa_2}$ indicate degradation of mRNA alone while sRNAs are recycled back. Further, here $r'_{p_1} = \frac{r_{p_1} k_1^+}{k_1^- + \sigma_1 + \kappa_1}$ and $r'_{p_2} = \frac{r_{p_2} k_2^+}{k_2^- + \sigma_2 + \kappa_2}$.

2. Moments

In this section, we list the results for first and second order moments obtained from the generating function approach. The results show that moments of a given order

involve higher order moments. In order to simplify our calculations, we consider moments up to second order and express the third order moments in terms of lower order moments using Gaussian approximation.

$$G_1 = \frac{r_s - g_1 G_{12} - g_2 G_{14}}{\gamma_s} \quad (\text{B6})$$

$$G_2 = \frac{r_{m_1} - (g_1 + d_1) G_{12}}{\gamma_{m_1}} \quad (\text{B7})$$

$$G_3 = \frac{r'_{p_1} G_{12}}{\gamma_{p_1}} \quad (\text{B8})$$

$$G_4 = \frac{r_{m_2}^0 + r_{m_2}^1 G_3 - (g_2 + d_2) G_{14}}{\gamma_{m_2}} \quad (\text{B9})$$

$$G_5 = \frac{r'_{p_2} G_{14}}{\gamma_{p_2}} \quad (\text{B10})$$

$$G_{11} = \frac{r_s G_1 - g_1 G_{112} - g_2 G_{114}}{\gamma_s} \quad (\text{B11})$$

$$G_{22} = \frac{r_{m_1} G_2 - (g_1 + d_1) G_{122}}{\gamma_{m_1}} \quad (\text{B12})$$

$$G_{33} = \frac{r'_{p_1} G_{123}}{\gamma_{p_1}} \quad (\text{B13})$$

$$G_{44} = \frac{r_{m_2}^0 G_4 + r_{m_2}^1 G_{34} - (g_2 + d_2) G_{144}}{\gamma_{m_2}} \quad (\text{B14})$$

$$G_{55} = \frac{r'_{p_2} G_{145}}{\gamma_{p_2}} \quad (\text{B15})$$

$$G_{12} = \frac{r_s G_2 + r_{m_1} G_1 - g_1 (G_{112} + G_{122}) - g_2 G_{124} - d_1 G_{112}}{\gamma_s + \gamma_{m_1} + g_1 + d_1} \quad (\text{B16})$$

$$G_{13} = \frac{r_s G_3 + r'_{p_1} (G_{12} + G_{112}) - g_1 G_{123} - g_2 G_{134}}{\gamma_s + \gamma_{p_1}} \quad (\text{B17})$$

$$G_{14} = \frac{r_s G_4 + r_{m_2}^0 G_1 + r_{m_2}^1 G_{13} - g_1 G_{124} - (g_2 + d_2) G_{114} - g_2 G_{144}}{\gamma_s + \gamma_{m_2} + g_2 + d_2} \quad (\text{B18})$$

$$G_{15} = \frac{r_s G_5 + r'_{p_2} (G_{14} + G_{114}) - g_1 G_{125} - g_2 G_{145}}{\gamma_s + \gamma_{p_2}} \quad (\text{B19})$$

$$G_{23} = \frac{r_{m_1} G_3 + r'_{p_1} (G_{12} + G_{122}) - (g_1 + d_1) G_{123}}{\gamma_{m_1} + \gamma_{p_1}} \quad (\text{B20})$$

$$G_{24} = \frac{r_{m_1} G_4 + r_{m_2}^0 G_2 + r_{m_2}^1 G_{23} - (g_1 + g_2 + d_1 + d_2) G_{124}}{\gamma_{m_1} + \gamma_{m_2}} \quad (\text{B21})$$

$$G_{25} = \frac{r_{m_1} G_5 + r'_{p_2} G_{124} - (g_1 + d_1) G_{125}}{\gamma_{m_1} + \gamma_{p_2}} \quad (\text{B22})$$

$$G_{34} = \frac{r'_{p_1} G_{124} + r_{m_2}^0 G_3 + r_{m_2}^1 (G_3 + G_{33}) - (g_2 + d_2) G_{134}}{\gamma_{p_1} + \gamma_{m_2}} \quad (\text{B23})$$

$$G_{35} = \frac{r'_{p_1} G_{125} + r'_{p_2} G_{134}}{\gamma_{p_1} + \gamma_{p_2}} \quad (\text{B24})$$

Using Gaussian approximation, we express the third order moments in terms of the lower order moments as shown below.

$$G_{112} = G_{11}G_2 + G_1G_2 + 2G_1G_{12} - 2G_1^2G_2 - G_{12} \quad (\text{B25})$$

$$G_{113} = G_{11}G_3 + G_1G_3 + 2G_1G_{13} - 2G_1^2G_3 - G_{13} \quad (\text{B26})$$

$$G_{114} = G_{11}G_4 + G_1G_4 + 2G_1G_{14} - 2G_1^2G_4 - G_{14} \quad (\text{B27})$$

$$G_{122} = G_{22}G_1 + G_1G_2 + 2G_2G_{12} - 2G_2^2G_1 - G_{12} \quad (\text{B28})$$

$$G_{123} = G_{12}G_3 + G_{13}G_2 + G_{23}G_1 - 2G_1G_2G_3 \quad (\text{B29})$$

$$G_{124} = G_{12}G_4 + G_{14}G_2 + G_{24}G_1 - 2G_1G_2G_4 \quad (\text{B30})$$

$$G_{125} = G_{12}G_5 + G_{15}G_2 + G_{25}G_1 - 2G_1G_2G_5 \quad (\text{B31})$$

$$G_{133} = G_{33}G_1 + G_1G_3 + 2G_3G_{13} - 2G_3^2G_1 - G_{13} \quad (\text{B32})$$

$$G_{134} = G_{13}G_4 + G_{14}G_3 + G_{34}G_1 - 2G_1G_3G_4 \quad (\text{B33})$$

$$G_{135} = G_{13}G_5 + G_{15}G_3 + G_{35}G_1 - 2G_1G_3G_5 \quad (\text{B34})$$

$$G_{144} = G_{44}G_1 + G_1G_4 + 2G_4G_{14} - 2G_4^2G_1 - G_{14} \quad (\text{B35})$$

$$G_{145} = G_{14}G_5 + G_{15}G_4 + G_{45}G_1 - 2G_1G_4G_5 \quad (\text{B36})$$

In order to see the effect of cross-talk, we have plotted the coefficient of variation for the target protein with r_{m_1} in the main text. In the absence of cross-talk (i.e. for $\sigma_1 = \sigma_2 = 0$), the coefficient of variation is significantly different showing no indication of optimal noise attenuation (see figure 8).

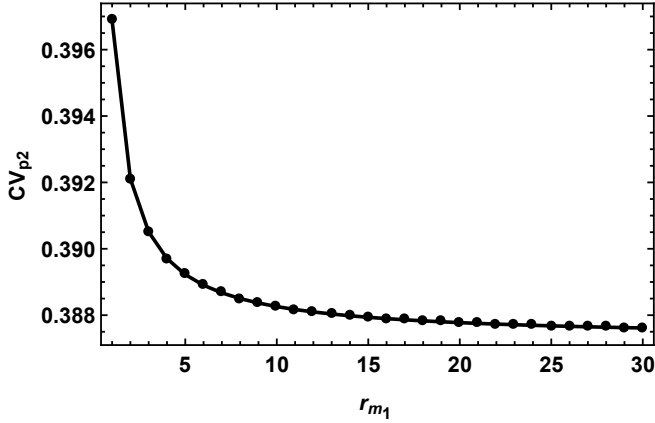


FIG. 8: Coefficient of variation for the target protein in the case of sFFL with $\sigma_1 = \sigma_2 = 0$. r_{m_1} represents m_1 synthesis rate. Here $r_s = 1$ and the other parameter values are same as those in figure 5.

Appendix C: Noise analysis for sCN

In the case of sCN, we follow the same master equation approach as done for sFFL. The master equation for

the probability of a given state is based on the following effective differential equations

$$\dot{s} = r_s - \gamma_s s - g_1 s m_1, \quad (\text{C1})$$

$$\dot{m}_1 = r_{m_1} - \gamma_{m_1} m_1 - d_1 s m_1 - g_1 s m_1, \quad (\text{C2})$$

$$\dot{p}_1 = r'_{p_1} s m_1 - \gamma_{p_1} p_1, \quad (\text{C3})$$

$$\dot{m}_2 = \frac{r_{m_2} k_c p_1}{1 + k_c p_1} - \gamma_{m_2} m_2, \quad (\text{C4})$$

$$\dot{p}_2 = r_{p_2} m_2 - \gamma_{p_2} p_2. \quad (\text{C5})$$

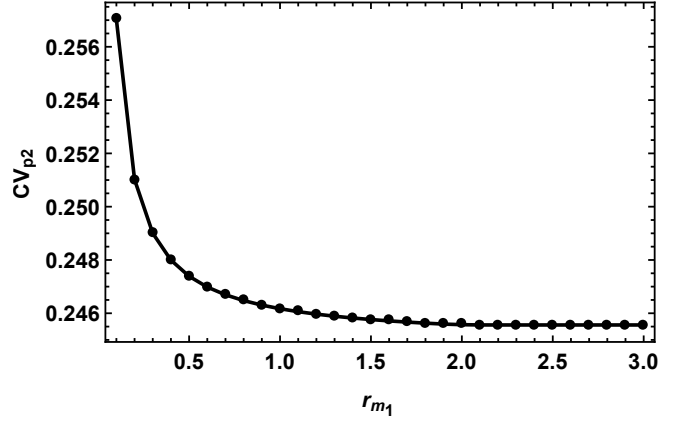


FIG. 9: Coefficient of variation for the target protein plotted with r_{m_1} in sCN. Here $r_s = 1$ and all other parameter values are same as those in figure 5. Further, in the case of sCN, $k_2^+ = k_2^- = \sigma_2 = \kappa_2 = 0$.

In figure 9, we plot the coefficient of variation $CV_{p_2} = (G_{55} + G_5 - G_5^2)^{1/2}/G_5$ with r_{m_1} . No minimum in the coefficient of variation is found in this case. Here $r_s = 1$ and all other parameter values are same as those in figure 5.

In the following, we present first and second moments necessary for obtaining the coefficient of variation for the sRNA-driven cascade network. As before, we use Gaussian approximation to express the third moments in terms of various first and second moments.

$$G_1 = \frac{r_s - g_1 G_{12}}{\gamma_s} \quad (\text{C6})$$

$$G_2 = \frac{r_{m_1} - (g_1 + d_1)G_{12}}{\gamma_{m_1}} \quad (\text{C7})$$

$$G_3 = \frac{r'_{p_1} G_{12}}{\gamma_{p_1}} \quad (\text{C8})$$

$$G_4 = \frac{r_{m_2}^0 + r_{m_2}^1 G_3}{\gamma_{m_2}} \quad (\text{C9})$$

$$G_5 = \frac{r_{p_2} G_4}{\gamma_{p_2}} \quad (\text{C10})$$

$$G_{11} = \frac{r_s G_1 - g_1 G_{112}}{\gamma_s} \quad (\text{C11})$$

$$G_{22} = \frac{r_{m_1} G_2 - (g_1 + d_1) G_{122}}{\gamma_{m_1}} \quad (\text{C12})$$

$$G_{33} = \frac{r'_{p_1} G_{123}}{\gamma_{p_1}} \quad (\text{C13})$$

$$G_{44} = \frac{r_{m_2}^0 G_4 + r_{m_2}^1 G_{34}}{\gamma_{m_2}} \quad (\text{C14})$$

$$G_{55} = \frac{r_{p_2} G_{45}}{\gamma_{p_2}} \quad (\text{C15})$$

$$G_{12} = \frac{r_s G_2 + r_{m_1} G_1 - g_1 (G_{112} + G_{122}) - d_1 G_{112}}{\gamma_s + \gamma_{m_1} + g_1 + d_1} \quad (\text{C16})$$

$$G_{13} = \frac{r_s G_3 + r'_{p_1} (G_{12} + G_{112}) - g_1 G_{123}}{\gamma_s + \gamma_{p_1}} \quad (\text{C17})$$

$$G_{14} = \frac{r_s G_4 + r_{m_2}^0 G_1 + r_{m_2}^1 G_{13} - g_1 G_{124}}{\gamma_s + \gamma_{m_2}} \quad (\text{C18})$$

$$G_{15} = \frac{r_s G_5 + r_{p_2} G_{14} - g_1 G_{125}}{\gamma_s + \gamma_{p_2}} \quad (\text{C19})$$

$$G_{23} = \frac{r_{m_1} G_3 + r'_{p_1} (G_{12} + G_{122}) - (g_1 + d_1) G_{123}}{\gamma_{m_1} + \gamma_{p_1}} \quad (\text{C20})$$

$$G_{24} = \frac{r_{m_1} G_4 + r_{m_2}^0 G_2 + r_{m_2}^1 G_{23} - (g_1 + d_1) G_{124}}{\gamma_{m_1} + \gamma_{m_2}} \quad (\text{C21})$$

$$G_{25} = \frac{r_{m_1} G_5 + r_{p_2} G_{24} - (g_1 + d_1) G_{125}}{\gamma_{m_1} + \gamma_{p_2}} \quad (\text{C22})$$

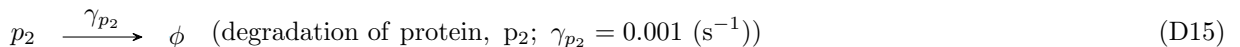
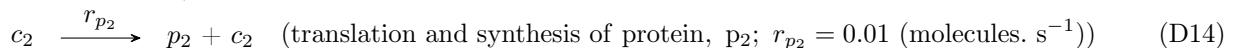
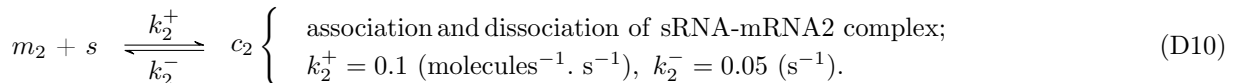
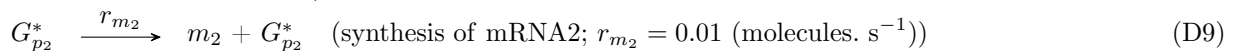
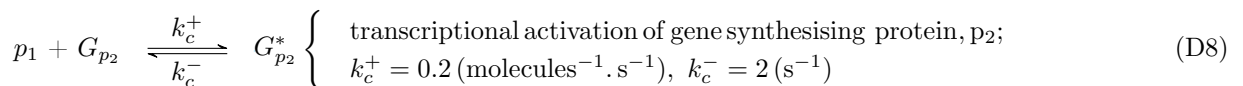
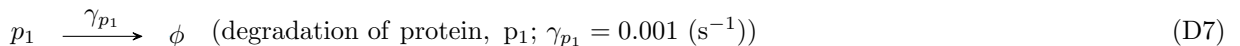
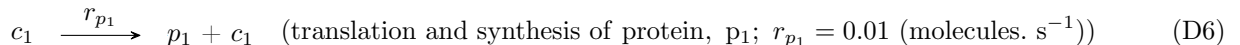
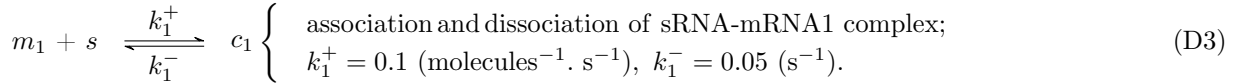
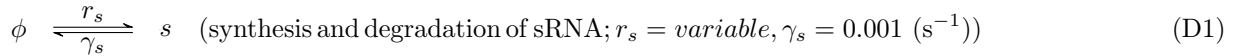
$$G_{34} = \frac{r'_{p_1} G_{124} + r_{m_2}^0 G_3 + r_{m_2}^1 (G_3 + G_{33})}{\gamma_{p_1} + \gamma_{m_2}} \quad (\text{C23})$$

$$G_{35} = \frac{r'_{p_1} G_{125} + r_{p_2} G_{34}}{\gamma_{p_1} + \gamma_{p_2}} \quad (\text{C24})$$

$$G_{45} = \frac{r_{m_2}^0 G_5 + r_{m_2}^1 G_{35} + r_{p_2} (G_4 + G_{44})}{\gamma_{m_2} + \gamma_{p_2}} \quad (\text{C25})$$

Appendix D: Stochastic simulations

The reactions considered for the stochastic simulations and the corresponding rates are listed below.



- [1] Storz G, Altuvia S and Wassarman K M 2005 An abundance of RNA regulators *Annu. Rev. Biochem.* **74** 199-217 (DOI: 10.1146/annurev.biochem.74.082803.133136)
- [2] Gottesman S 2005 Micros for microbes: non-coding regulatory RNAs in bacteria *Trends Genet.* **21** 399-404 (DOI: 10.1016/j.tig.2005.05.008)
- [3] Frohlich K S and Papenfort K 2016 Interplay of regulatory RNAs and mobile genetic elements in enteric pathogens *Mol. Microbiol.* **101** 701-13 (DOI: 10.1111/mmi.13428)
- [4] Soper T, Mandin P, Majdalani N, Gottesman S and Woodson S A 2010 Positive regulation by small RNAs and the role of Hfq *Proc. Natl. Acad. Sci. USA* **107** 9602-07 (DOI: 10.1073/pnas.1004435107)
- [5] Levine E, Zhang Z, Kuhlman T and Hwa T 2007 Quantitative characteristics of gene regulation by small RNA *PLoS Biol.* **5** e229 (DOI: 10.1371/journal.pbio.0050229)
- [6] Pal M, Ghosh S and Bose I 2016 Functional characteristics of gene expression motifs with single and dual strategies of regulation *Biomed. Phys. Eng. Express* **2** 025009 (DOI: 10.1088/2057-1976/2/2/025009)
- [7] Raj A and van Oudenaarden A 2008 Nature, nurture, or chance: Stochastic gene expression and its consequences *Cell* **135** 216-26 (DOI: 10.1016/j.cell.2008.09.050)
- [8] Chalancon G, Ravarani C N J, Balaji S, Martinez-Arias A, Aravind L, Jothi R and Babu M M 2012 Interplay between gene expression noise and regulatory network architecture *Trends Genet.* **28** 221-32 (DOI: 10.1016/j.tig.2012.01.006)
- [9] Shimoni Y, Friedlander G, Hetzroni G, Niv G, Altuvia S, Biham O and Margalit H 2007 Regulation of gene expression by small non-coding RNAs: a quantitative view *Mol. Syst. Biol.* **3** 1-9 (DOI: 10.1038/msb4100181)
- [10] Osella M, Bosia C, Cora D and Caselle M 2011 The role of incoherent microRNA-mediated feed-forward loops in noise buffering *PLoS Comput. Biol.* **7** e1001101 (DOI: 10.1371/journal.pcbi.1001101)
- [11] Tej S, Gaurav K and Mukherji S 2019 Small RNA driven feed-forward loop: critical role of sRNA in noise filtering *Phys. Biol.* **16** 1-16 (DOI: 10.1088/1478-3975/ab1563)
- [12] Bosia C, Pagnani A and Zecchina R 2013 Modelling competing endogenous RNA networks *PLoS One* **8** e66609

- 1-12 (DOI: 10.1371/journal.pone.0066609)
- [13] Figliuzzi M, Marinari E and De Martino A 2013 MicroRNAs as selective channel of communication between competing RNAs: steady state theory *Biophys. J.* **104** 1203-13 (DOI: 10.1016/j.bpj.2013.01.012.)
- [14] Bossi L and Figueroa-Bossi N 2016 Competing endogenous RNAs: a target-centric view of small RNA regulation in bacteria *Nat. Rev. Microbiol.* **14** 775-84 (DOI: 10.1038/nrmicro.2016.129)
- [15] Martirosyan A, Figliuzzi M, Marinari E and De Martino A 2016 Probing the limits to microRNA-mediated control of gene expression *PLoS Comput. Biol.* **12** e1004715. (DOI:10.1371/journal.pcbi.1004715)
- [16] Martirosyan A, De Martino A, Pagnani A and Marinari E 2017 ceRNA crosstalk stabilizes protein expression and affects the correlation pattern of interacting proteins *Sci. Rep.* **7** 1-11 (DOI: 10.1038/srep43673)
- [17] Alon U 2006 *An introduction to systems biology: design principles of biological circuits* (London, UK: Chapman and Hall/CRC)
- [18] Papenfort K, Espinosa E, Casadesus J and Vogel J 2015 Small RNA-based feedforward loop with AND-gate logic regulates extrachromosomal DNA transfer in Salmonella *Proc. Natl. Acad. Sci. USA* **112** E4772-81 (DOI: 10.1073/pnas.1507825112)
- [19] Riba A, Bosia C, El Baroudi M, Ollino L and Caselle M 2014 A combination of transcriptional and microRNA regulation improves the stability of the relative concentrations of target genes *PLoS Comput. Biol.* **10** e1003490 (DOI: 10.1371/journal.pcbi.1003490)
- [20] Cora D, Re A, Caselle M and Bussolino F 2017 MicroRNA-mediated regulatory circuits: outlook and perspectives *Phys. Biol.* **14** 045001-11 (DOI: 10.1088/1478-3975/aa6f21)
- [21] Majdalani N, Hernandez D and Gottesman S 2002 Regulation and mode of action of the second small RNA activator of RpoS translation, RprA *Mol. Microbiol.* **46** 813-26 (DOI: 10.1046/j.1365-2958.2002.03203.x)
- [22] van Kampen N G 2007 *Stochastic processes in physics and chemistry* (Amsterdam: Elsevier)
- [23] Lafuerza L F and Toral R 2010 On the Gaussian approximation for master equations *J. Stat. Phys.* **140** 917-33 (DOI: 10.1007/s10955-010-0024-7)
- [24] Gillespie D T 1976 A general method for numerically simulating the stochastic time evolution of coupled chemical reactions *J. Comput. Phys.* **22** 403-34 (DOI: 10.1016/0021-9991(76)90041-3)
- [25] Gillespie D T 1977 Exact stochastic simulation of coupled chemical reactions *J. Phys. Chem.* **81** 2340-61 (DOI: 10.1021/j100540a008)